

Analysis of Traveling Ionospheric Disturbances (TIDs) in GPS TEC Launched by the 2011 Tohoku Earthquake

Geoff Crowley, Irfan Azeem, Adam Reynolds, Tim Duly, Patrick McBride, Clive Winkler and Don Hunton

ASTRA
5777 Central Ave., Suite 221
Boulder, CO 80301
USA

ABSTRACT

TIDs have been detected using various measurement techniques, including HF sounders, incoherent scatter radars, in-situ measurements, and optical techniques. However, there is still much we do not yet know or understand about TIDs. Observations of TIDs have tended to be sparse, and there is a need for additional observations to provide new scientific insight into the geophysical source phenomenology and wave propagation physics. The dense network of GPS receivers around the globe offers a relatively new data source to observe and monitor TIDs. In this paper, we use Total Electron Content (TEC) measurements from 4000 GPS receivers throughout the continental United States to observe TIDs associated with the 11 March 2011 Tohoku tsunami. The tsunami propagated across the Pacific to the US west coast over several hours, and corresponding TIDs were observed over Hawaii, and via the network of GPS receivers in the US. The network of GPS receivers in effect provides a 2D spatial map of TEC perturbations, which can be used to calculate TID parameters, including horizontal wavelength, speed, and period. Well-formed, planar traveling ionospheric disturbances were detected over the west coast of the US ten hours after the earthquake. Fast Fourier transform analysis of the observed waveforms revealed that the period of the wave was 15.1 minutes with a horizontal wavelength of 194.8 km, phase velocity of 233.0 m/s, and an azimuth of 105.2° (propagating nearly due east in the direction of the tsunami wave). These results are consistent with TID observations in airglow measurements from Hawaii earlier in the day, and with other GPS TEC observations. The vertical wavelength of the TID was found to be 43.5 km. The TIDs moved at the same velocity as the tsunami itself. Much work is still needed in order to fully understand the ocean-atmosphere coupling mechanisms, which could lead to the development of effective tsunami detection/warning systems. The work presented in this paper demonstrates a technique for the study of ionospheric perturbations that can affect navigation, communications and surveillance systems.

1. INTRODUCTION

The major source of error in geolocation is Traveling Ionospheric Disturbances (TIDs), both for long ranges (OTHR) and short ranges (HFDF). TIDs are perturbations in ionospheric electron density caused by atmospheric gravity waves (AGWs) via ion-neutral collisions as they travel through the thermosphere/ionosphere from their source region. At ionospheric heights, the motion of the neutral gas in the AGW sets the ionosphere into motion. Thus, the signature of the AGW is manifested as variations of electron density in the ionosphere, resulting in a TID. As a result of these ionospheric perturbations, TIDs have been detected by various radio techniques for many years, including ionosondes, incoherent scatter radars, and HF Doppler sounders. HF sounder measurements of TIDs have been presented by a number of authors [e.g. Crowley, 1985; Waldock and Jones, 1987; Crowley et al., 1987; Crowley and McCrea, 1988;

Crowley and Rodrigues, 2012; and included references]. A newer technique for measuring TIDs is the use of GPS total electron content (TEC), which is the focus of this paper.

AGWs are buoyancy waves generated as a consequence of gravity attempting to restore the equilibrium of an atmospheric perturbation [Hines, 1960; Yeh, 1974; Francis, 1975]. There are many different generation mechanisms for AGWs. In the auroral regions they can be caused by Joule heating associated with geomagnetic storms [e.g., Richmond 1978; Hunsucker 1982]. Severe meteorological events, such as thunderstorms and tornadoes, and tropospheric deep convection cells [Fovell et al., 1992; Alexander et al., 1995; Lane et al. 2001] have been shown to generate AGWs and their signatures have been recorded in the thermosphere [Taylor and Hapgood., 1988; Nishioka et al., 2013]. Several studies have suggested that convective storms are one of the primary drivers for AGWs that propagate upward into the mesopause region [Alexander, 1996; Holton and Alexander, 1999; Walterscheid et al. 2001]. AGWs can also be man-made, as nuclear detonations have been shown to launch the waves into Earth's atmosphere [Row, 1967]. AGWs transport energy and momentum upward and are a prime example of coupling from lower atmospheric processes (i.e., in the troposphere) into the upper atmosphere (i.e., in the thermosphere/ionosphere).

Natural disasters, including earthquakes [Hasbi et al., 2011 and references therein], and tsunamis [Makela et al., 2011] have also generated AGWs and associated ionospheric signatures such as TIDs. The March 11, 2011 Tohoku earthquake and subsequent tsunami off the east of Japan created AGWs which propagated on global spatial scales. The signature of the AGWs was observed with airglow imagers located in Maui, Hawaii [Makela et al., 2011]. In their study, Makela et al. (2011) observed AGWs that were consistent with numerical modeling of AGWs generated by an earthquake. Occhipinti et al [2013] reviewed far-field measurements of earthquake-related ionospheric signatures and also presented near-field GPS-based total electron content (TEC) measurements associated with the Tohoku event. Komjathy et al [2012] also reported on the Tohoku earthquake and the ionospheric signatures that resulted from it. They showed that a global network of GPS receivers was able to detect the earthquake, but they did not include measurements at specific positions across the globe to give indications of the motion or velocity of the TEC disturbances. For the same catastrophic event, spatially resolved measurements of TEC variations, measured with a network of GPS receivers in Japan and Taiwan, revealed an initial ionospheric TEC enhancement about 7 minutes after the earthquake located at an "ionospheric epicenter" about 200 km distant from the geologic epicenter [Tsugawa, et al, 2011; Liu, et al, 2011]. Concentric rings of TEC enhancements and depletions then propagated radially outward from this ionospheric epicenter. Tsugawa et al. [2011] reported velocities in the range 138-3,457 m/s, while Liu et al. [2011] observed initial velocities of 2,300-3,300 m/s and later detected concentric rings with a lower velocity close to the tsunami wave velocity of 200 – 222 m/s. The tsunami propagated across the Pacific to the US west coast over several hours, and corresponding TIDs were observed over Japan [Galvan et al., 2012; Saito et al., 2011; Maruyama et al., 2011].

In this paper, we extend the spatially-resolved measurements near Japan to the continental United States. We analyze TEC measurements from various GPS receivers throughout the US to observe TIDs associated with the March 11, 2011 Tohoku earthquake and tsunami. The network of GPS receivers provides a 2D spatial map of TEC perturbations, which we have used to calculate TID parameters, including horizontal wavelength, speed, and period. The results presented here are consistent with the previous studies of TIDs associated with the Tohoku event. Although coupling between the ocean and ionosphere associated with tsunamis was predicted as early as the 1970s, much work is still needed in order to fully understand the geophysical source phenomenology, the ocean-atmosphere coupling mechanisms, and the wave propagation physics, all of which are necessary for the development of effective tsunami detection/warning systems based on ionospheric monitoring.

2. GPS TEC DATA

We used GPS TEC data from over 4000 sites in the United States to detect and image TIDs. Our approach to processing the GPS data to derive vertical TEC maps was similar to that presented by Tsugawa et al. [2007] and Nishioka et al. [2013]. In brief, we used the pseudorange and phase measurements of GPS signals at L1(1575.42 MHz) and L2 (1227.6 MHz) frequencies to derive slant TEC values which were then converted to

vertical TEC (VTEC) using the obliquity factor model described by Kaplan and Hagerty [2006]. In mapping slant TEC to VTEC we assumed the ionospheric pierce point (IPP) altitude to be 350 km. We then computed perturbations in TEC by detrending VTEC using a 20-minute running mean for each PRN followed by horizontal smoothing of the resulting TEC map using a 2D Gaussian filter as described by Nishioka et al. [2013].

3. RESULTS

A magnitude 9.0 earthquake occurred on March 11, 2011 at 05:46:23 Universal Time (UT) near the northeast coast of Honshu, Japan. The earthquake spawned a tsunami that resulted in widespread destruction along the coast of the northern part of Japan and threatened coastal areas throughout the Pacific. Figure 1 shows the NOAA Method of Splitting Tsunami model (MOST) simulation of the 2011 Tohoku tsunami source and water heights over a tsunami travel time (TTT) map. The Tohoku tsunami propagated throughout the Pacific Ocean reaching the entire Pacific coast of North and South America from Alaska to Chile. Warnings were issued and evacuations carried out in many countries bordering the Pacific. While the tsunami affected many of these places, the extent of damage on the eastern side of the Pacific was minor. Chile's Pacific coast, one of the furthest from Japan at about 17,000 km (11,000 mi) distant, was struck by waves 2 m (6.6 ft) high, compared with an estimated wave height of 38.9 meters (128 ft) at Omoe peninsula, Miyako city, Japan. The simulation in Figure 1 predicts the tsunami reached the west coast of the United States about 10 to 11 hours after the earthquake struck Japan.

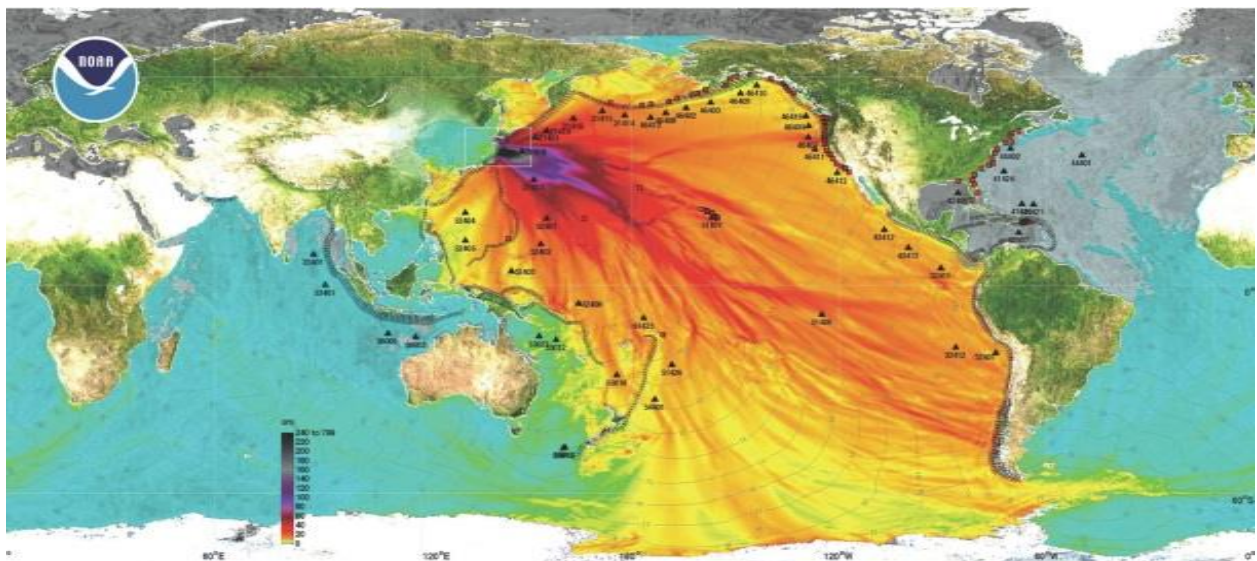


Figure 1. NOAA model amplitudes for the 2011 Tohoku tsunami calculated with the Method of Splitting Tsunami (MOST) forecast model. Filled colors show maximum computed tsunami amplitude in cm during 24 hours of wave propagation. Contour lines show computed tsunami arrival time. Source: http://nctr.pmel.noaa.gov/honshu20110311/Energy_plot20110311_ok.jpg

Figure 2 shows the results of our GPS TEC analysis. We show six GPS TEC maps over the continental US on March 11, 2011 at times between 15:00 and 19:30 UTC to illustrate the extent and propagation of the TIDs. The TEC perturbation scale in Figure 2 is ± 0.03 TECU ($1 \text{ TECU} = 1 \times 10^{16} \text{ \#/m}^2$). At 15:00, no indication of TIDs in the northwest region can be seen. TIDs were first seen in the GPS TEC measurements at 15:46 UT, and by 16:40 UTC, planar wavefronts above the US West Coast had clearly formed with local orientation in a North East-South West direction. These TID wave trains are also present in the TEC map at 17:00 UTC. At 18:00 UT, the wave trains were breaking up and by 19:30 they had largely dissipated. A full

TEC map sequence (not shown here) at a cadence of 30 seconds shows that these TID wavefronts propagate from the direction of the earthquake at an azimuth of 101° . In total, the TIDs persisted for about 4 hours after they were first seen. We performed a 3D Fast Fourier Transform (FFT) analysis on the GPS TEC dataset to calculate various TID wave parameters. Based on the FFT analysis we estimate the TID period to be 15.1 minutes, the horizontal wavelength to be 198 km, and the phase velocity to be 216 m/s. The total horizontal distance from the earthquake epicenter to central Washington is approximately 7,500 km. The delay between the earthquake (5:46 UTC) and the first detection of TIDs in the northwest (15:46 UTD) was ten hours. These two results combine to give an average speed of 208 m/s, in good agreement with the FFT analysis. The speed is also in excellent agreement with the measurements of Liu, et al [2011].

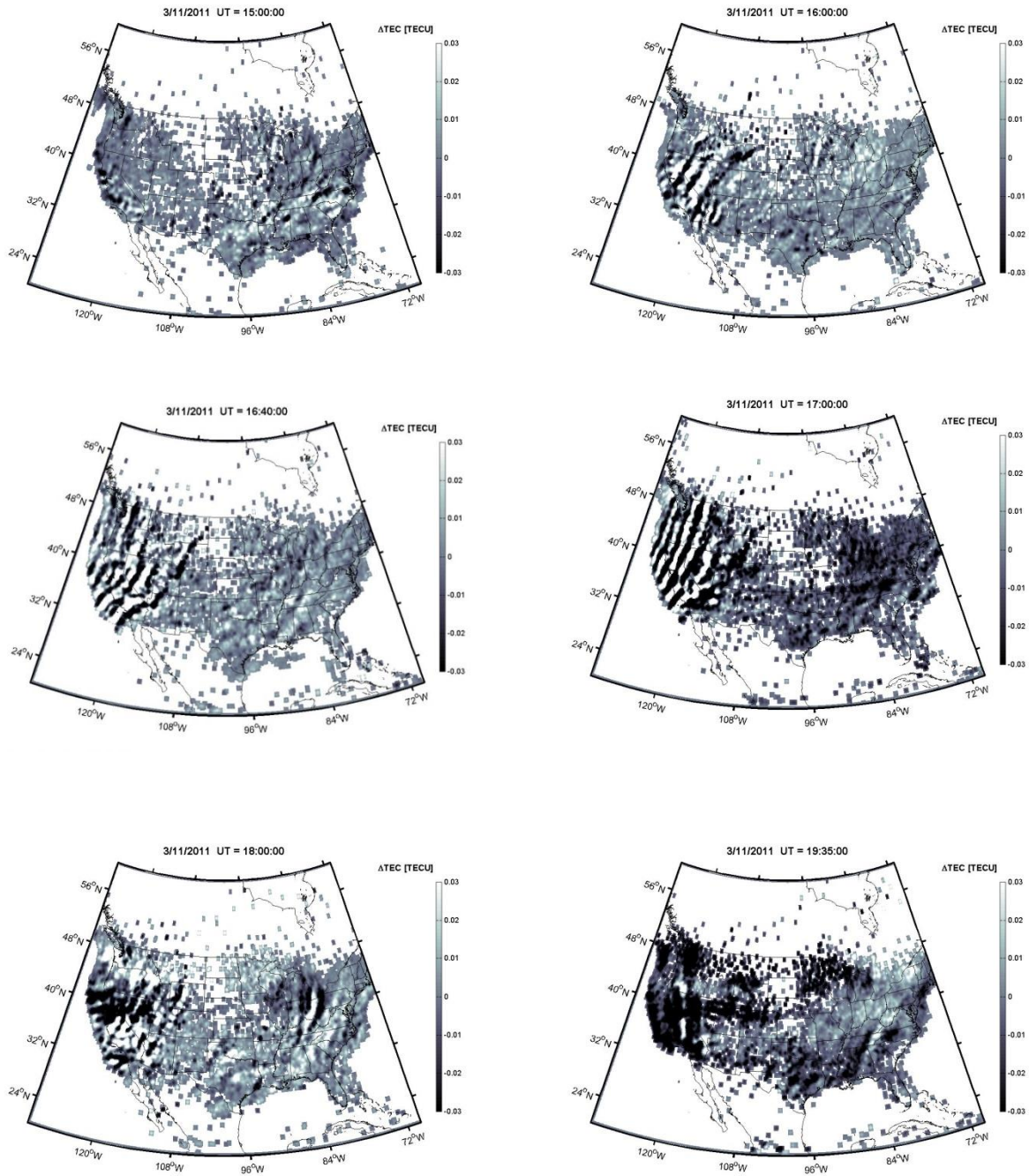


Figure 2. 2D maps of TEC perturbations between 15:00 UT and 19:35 UT. These maps show the planar wavefronts of a TID over the west coast of United States.

In Figure 3a, a subset of data was selected covering the Western United States of $\sim 4^\circ \times 4^\circ$ in latitude and longitude, which is approximately 460 x 350 km at the ionospheric pierce point. Within this region, a 2 hour time window was selected from 17:03:30 to 19:03:30 UTC, representative of the TID passing through this region. A 3D FFT was calculated for this 3D “block,” and the data are zero padded to provide interpolation in the frequency domain. From this calculation, the maximum amplitude was found, and Figure 3b shows the k_x vs. k_y “slice” of the maximum value of the FFT, which is equivalent to $\lambda=194.8$ km and $\theta=105.2^\circ$ (measured positive clockwise from North). Next, Figure 3c shows the FFT of the third dimension (i.e., time) of the 3D FFT block, and shows the maximum value at 0.011 Hz ($T=15.1$ minutes). Finally, Figure 3d shows a snapshot of the wave recovered from the analysis, representative of the wave shown in Figure 3a.

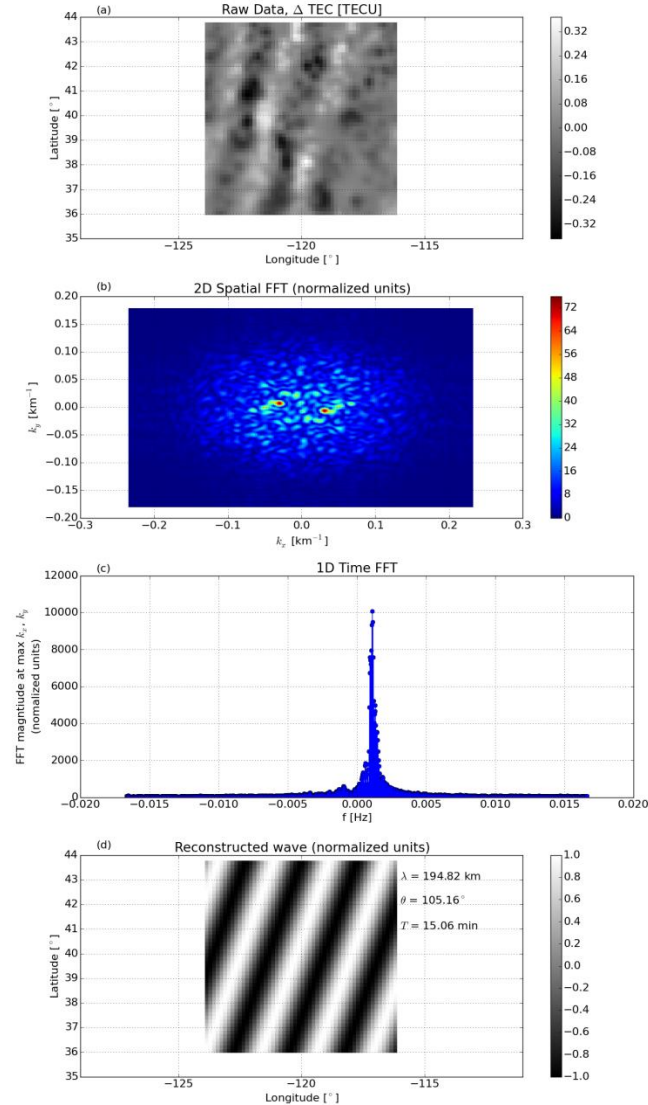


Figure 3. 3D FFT analysis for the TID passing over the Western US. (a) Selected raw data. The max amplitude of the FFT is calculated, and the (b) spatial slice and (c) time frequencies are plotted. (d) The reconstructed wave is shown from the 3D FFT analysis.

Next we use the Boussinesq dispersion relation to estimate the vertical wavelenghts, λ_z of the TID. We use the dispersion relation as described by Vadas and Crowley [2010]:

$$\omega_{Ir}^2 = \frac{k_H^2 N^2}{m^2 + k_H^2} \quad (1)$$

where ω_{Ir}^2 is the intrinsic frequency of the wave, k_H is the horizontal wave number, N is Brunt-Väisälä frequency, and m is the vertical wavenumber ($m=2\pi/\lambda_z$). The relationship between the observed (ω_r) and intrinsic frequencies is given by:

$$\omega_r = \omega_{Ir} + k_x u + k_y v \quad (2)$$

where:

k_x = Zonal wave number, k_y = Meridional wave number, u = Zonal neutral wind, and v = Meridional neutral wind.

We use the Thermosphere-Ionosphere-Mesosphere Electrodynamics General Circulation Model (TIME-GCM) [Roble and Ridley, 1994] to estimate neutral winds and Brunt-Väisälä frequency at the time and location of the observed TIDs. The model zonal and meridional winds at 18 UT and at 40° N and 120° W were -143 m/s and -15 m/s, respectively. Using these values, we find that $\lambda_z = 43.5$ km.

4. CONCLUSIONS

In this paper, we used total electron content (TEC) measurements from 4,000 GPS receivers throughout the continental United States to image, as far as we know for the first time, TIDs over the US associated with the 11 March 2011 Tohoku tsunami. The tsunami propagated across the Pacific to the Western Coast of the US over a ten-hour period where corresponding TIDs were observed in ionospheric TEC measurements. We use a 3D FFT analysis on a sequence GPS TEC images over the US to derive TID wave parameters. The period of the wave was 15.1 minutes with a horizontal wavelength of 194.8 km, phase velocity of 233.0 m/s, and an azimuth of 105.2° (propagating in the direction of the tsunami wave). These results are consistent with TID observations in airglow measurements from Hawaii earlier in the day, and other GPS TEC observations. The vertical wavelength of the TID was found to be 43.5 km. This paper demonstrates that the 2011 tsunami generated trans-Pacific TIDs which persisted for about 4 hours over North America. The coincidence of the tsunami travel time across the Pacific and the delay in the appearance of TIDs in North America suggests a coupling between the tsunami and the ionospheric response throughout the propagation of the ocean waves.

ACKNOWLEDGEMENTS

The authors acknowledge contract N00014-13-1-0343 from the Office of Naval Research, and subcontract NWRA-12-S-151 (under NASA Contract NNH12CE58C to NWRA).

REFERENCES

- Alexander, M. J., J. R. Holton, and D. R. Durran (1995), The gravity wave response above deep tropical convection in a squall line simulation, *J. Atmos. Sci.*, 52(12), 2212 – 2226.
- Alexander, M. J., (1996), A simulated spectrum of convectively generated gravity waves: Propagation from the tropopause to the mesopause and effects on the middle atmosphere. *J. Geophys. Res.*, 101, 1571-1588.
- Crowley, G. (1985), Doppler radar studies of the Antarctic ionosphere, PhD thesis, Univ. of Leicester, Leicester, U. K.
- Crowley, G., and I. W. McCrea (1988), A synoptic study of TIDs observed in the UK during the first WAGS campaign, October 10–18, 1985, *Radio Sci.*, 23, 905–917, doi:10.1029/RS023i006p00905.

- Crowley, G., and F. S. Rodrigues (2012), Characteristics of traveling ionospheric disturbances observed by the TIDDBIT sounder, *Radio Sci.*, 47, RS0L22, doi:10.1029/2011RS004959.
- Crowley, G., T. B. Jones, and J. R. Dudeney (1987), Comparison of short period TID morphologies in Antarctica during geomagnetically quiet and active intervals, *J. Atmos. Terr. Phys.*, **49**, 1155–1162, doi:10.1016/0021-9169(87)90098-5.
- Fovell, R., D. Durran, and J. R. Holton, (1992), Numerical simulations of convectively generated stratospheric gravity waves. *J. Atmos. Sci.*, 49, 1427–1442.
- Francis, S. H. (1975), Global propagation of atmospheric gravity waves: a review *Journal of Atmospheric and Solar-Terrestrial Physics*, 37 (1975), p. 1011.
- Galvan, D. A., A. Komjathy, M. P. Hickey, P. Stephens, J. Snively, Y. Tony Song, M. D. Butala, and A. J. Mannucci (2012), Ionospheric signatures of Tohoku-Oki tsunami of March 11, 2011: Model comparisons near the epicenter, *Radio Sci.*, 47, RS4003, doi:10.1029/2012RS005023.
- Hasbi, A. M., Mohd Ali, M. A., and Misran, N.(2011), Ionospheric variations before some large earthquakes over Sumatra, *Nat. Hazards Earth Syst. Sci.*, 11, 597–611, doi:10.5194/nhess-11-597-2011.
- Hines, C. O. (1960). Internal atmospheric gravity waves at ionospheric heights, *Can. J. Phys.*, 38, 1441.
- Holton, J. R., and M. J. Alexander (1999), Gravity waves in the mesosphere generated by tropospheric convection, *Tellus A-B*, 51, 45 – 58.
- Hunsucker, R. D. (1982), Atmospheric gravity waves generated in the high-latitude ionosphere: A review, *Rev. Geophys.*, 20(2), 293–315, doi:10.1029/RG020i002p00293.
- Kaplan, E. D., and C. Hagerty, (2006), *Understanding GPS: Principles and Applications*, 2nd Ed., Artech House.
- Komjathy, A., D. A. Galvan, P. Stephens, M. D. Butala, V. Akopian, B. Wilson, O. Verkhoglyadova, A. J. Mannucci, and M. Hickey (2012), Detecting ionospheric TEC perturbations caused by natural hazards using a global network of GPS receivers: The Tohoku case study, *Earth Planets Space*, **64**, 1287–1294.
- Lane, T. P., Reeder, M. J. and Clark, T. L. (2001), Numerical modeling of gravity wave generation by deep tropical convection. *J. Atmos. Sci.*, 58, 1249–1274.
- Liu, J. - Y., C. - H. Chen, C. - H. Lin, H. - F. Tsai, C. - H. Chen, and M. Kamogawa (2011), Ionospheric disturbances triggered by the 11 March 2011 M9.0 Tohoku earthquake, *J. Geophys. Res.*, 116, A06319, doi:10.1029/2011JA016761.
- Makela, J. J., et al. (2011), Imaging and modeling the ionospheric airglow response over Hawaii to the tsunami generated by the Tohoku earthquake of 11 March 2011, *Geophys. Res. Lett.*, 38, L13305, doi:10.1029/2011GL047860.
- Maruyama, T., T. Tsugawa, H. Kato, A. Saito, Y. Otsuka, and M. Nishioka, Ionospheric multiple stratifications and irregularities induced by the 2011 off the Pacific coast of Tohoku Earthquake (2011), *Earth Planets Space*, **63**, 869–873.
- Nishioka, M., T. Tsugawa, M. Kubota, and M. Ishii (2013), Concentric waves and short-period oscillations observed in the ionosphere after the 2013 Moore EF5 tornado, *Geophys. Res. Lett.*, 40, 5581–5586, doi:10.1002/2013GL057963.
- Occhipinti, G., L. Rolland, P. Lognonne´, and S. Watada (2013), From Sumatra 2004 to Tohoku-Oki 2011: The systematic GPS detection of the ionospheric signature induced by tsunamigenic earthquakes, *J. Geophys. Res. Space Physics*, 118, doi:10.1002/jgra.50322.
- Richmond, A.D. (1978), Gravity wave generation, propagation, and dissipation in the thermosphere, *J. Geophys. Res.*, 83, 4131.

- Roble, R. G., and E. C. Ridley (1994), A thermosphere-ionosphere-mesosphere electrodynamic general circulation model (TIME-GCM): Equinox solar cycle minimum simulations (30-500 km), *Geophys. Res. Lett.*, 21, 417-420.
- Row, R. V. (1967), Acoustic-gravity waves in the upper atmosphere due to a nuclear detonation and an earthquake, *J. Geophys. Res.*, 72, 1599–1610.
- Saito, A., T. Tsugawa, Y. Otsuka, M. Nishioka, T. Iyemori, M. Matsumura, S. Saito, C. H. Chen, Y. Goi, and N. Choosakul (2011), Acoustic resonance and plasma depletion detected by GPS total electron content observation after the 2011 off the Pacific coast of Tohoku Earthquake, *Earth Planets Space*, 63, 863–867.
- Taylor, M. J., and H. A. Hapgood (1988), Identification of a thunderstorm as a source of short period gravity waves in the upper atmospheric nightglow emissions, *Planet. Space Sci.*, 36, 975 – 985.
- Tsugawa, T., Otsuka, Y., Coster, A. J., and Saito, A. (2007), Medium-scale traveling ionospheric disturbances detected with dense and wide TEC maps over North America, *Geophys. Res. Lett.*, 34, L22101, doi:10.1029/2007GL031663.
- Tsugawa, et al, 2011 Tsugawa, T., A. Saito, Y. Otsuka, M. Nishioka, T. Maruyama, H. Kato, T. Nagatsuma, and K. T. Murata (2011), Ionospheric disturbances detected by GPS total electron content observation after the 2011 off the Pacific coast of Tohoku Earthquake, *Earth Planets Space*, 63, 875–879.
- Vadas, S. L., and G. Crowley (2010), Sources of the traveling ionospheric disturbances observed by the ionospheric TIDDBIT sounder near Wallops Island on 30 October 2007, *J. Geophys. Res.*, 115, A07324, doi:10.1029/2009JA015053.
- Waldock, J. A., and T. B. Jones (1987), Source regions of medium scale travelling ionospheric disturbances observed at mid-latitudes, *J. Atmos. Terr. Phys.*, 49, 105–114, doi:10.1016/0021-9169(87)90044-4.
- Walterscheid, R. L., G. Schubert, D.G. Brinkman (2001), Small scale gravity waves in the upper mesosphere and lower thermosphere generated by deep tropical convection, *J. Geophys. Res.*, 106 (31), pp. 825–31832.
- Yeh K. C., C.H. Liu (1974), Acoustic gravity waves in the upper atmosphere, *Reviews of Geophysics and Space Physics*, 12, p. 193.